J Mater Sci (2008) 43:5546–5550
DOI 10.1007/s10853-008-2825-5

Thermal equation of state of natural chromium spinel up to 26.8 GPa and 628 K

Dawei Fan · Wenge Zhou · Chongqiang Liu · Yonggang Liu · Xi Jiang · Fang Wan · Jing Liu · Xiaodong Li · Hongsen Xie

Received: 4 December 2007 / Accepted: 20 June 2008 / Published online: 9 July 2008

Abstract A pressure–volume–temperature data set has been obtained for natural chromium spinel, using synchrotron X-ray diffraction with a resistance heated diamond-anvil cell (RHDAC). The unit cell parameter of the chromium spinel was measured by energy dispersive X-ray diffraction up to pressures of 26.8 GPa and temperatures of 628 K. No phase change has been observed. The observed P–V–T data were fit to the high-temperature Birch-Murnaghan equation of state, with V_0 fixed at its experimental value, yields $K_0 = 209 \pm 9$ GPa, $(\partial K/\partial T)_P = -0.056 \pm 0.035$ GPa K^{-1}, and $\alpha_0 = 7 \pm 1 \times 10^{-5}$ K^{-1}. The temperature derivative of the bulk modulus $(\partial K/\partial T)_P$ of chromium spinel is determined here for the first time. The obtained K_0 is slightly higher than the previous results of synthetic spinel. We suggest that Fe^{2+}–Mg^{2+} substitution is responsible for the high bulk modulus of chromium spinel.

D. Fan · W. Zhou (✉) · Y. Liu · F. Wan · H. Xie
Institute of Geochemistry, Chinese Academy of Science, Guiyang 550002, China
e-mail: wengezhou67@163.com

D. Fan
e-mail: fandawei1982@126.com

D. Fan · F. Wan
Graduate University of Chinese Academy of Science, Beijing 100049, China

C. Liu
Institute of Geochemistry, Chinese Academy of Science, Guiyang 550002, China

X. Jiang
College of Resource and Environment Engineering of Guiozhou University, Guiyang 550003, China

J. Liu · X. Li
Institute of High Energy Physics, Chinese Academy of Science, Beijing 100049, China

Introduction

Spinel (AB_2O_4, where, in most cases, A is a divalent and B a trivalent cation) have a close-packed face-centered cubic structure with space group $Fd\bar{3}m$. The unit cell contains 32 O atoms in cubic close packing, 16 octahedral sites (M), and 8 tetrahedral sites (T) occupied by the A and B cations.

Spinel oxides form an important range of ceramic compounds with great interesting electrical, mechanical, magnetic, and optical properties, thus suitable for various technological applications, such as superconductors, magnetic cores, and high-frequency devices [1–3]. Since many of the spinels are common minerals, they also have great geological and geophysical interest [4–6]; especially chromium spinel is regarded as important petrogenetic indicator in ultramafic to mafic rocks [6].

Recently, different high-pressure studies of spinel focused on phase stability and EOS of synthetic spinel [7–29]. Most of these studies showed that spinel split into periclase (MgO) and corundum (Al_2O_3) at about 15 GPa and 1273 K [7, 8]. However, Liu [9] reported a dense phase of spinel at 25 GPa and 1273 K, which was called ε-$MgAl_2O_4$. Based on their experimental results, Irifune et al. [7] argued that the spinel is unable to form the ε-$MgAl_2O_4$ up to 26 GPa and 1773 K, but to form the high-pressure phase of $CaFe_2O_4$ structure. The experimental results of Funamori et al. [8] and Akaogi et al. [11] supported the conclusions of the Irifune coauthors [7]. However, most of studies focused on synthetic samples, only a few of works regard natural spinels [16, 30], which

can help us to verify the quality of the models of the effect of compositional variability in such mineral families.

P–V–T relationship for a chromium spinel up to 14.8 GPa and 603 K has been reported by Ma et al. [30]. However, the pressure range explored in their study is smaller, and the retrieved bulk modulus, $K_0 = 396$ GPa is substantially larger than in previous studies (181.5–217 GPa) [14–29]. In this paper, we reported the thermal EOS of the same chromium spinel up to 26.8 GPa and 628 K, and derived the thermodynamic and thermoelastic parameters.

Experimental procedures

Samples

The natural spinel was selected from a lherzolite xenolith collected from Hannuoba basalt, Hebei provinces, north China. Its impurity content is less than 1%. The chemical composition of the spinel was determined by electron probe [30], and chemical formula of the crystal was calculated to be $(Na^{+}Mg^{2+}Fe^{2+}Ti^{4+})_{0.9661}(Cr^{3+}Al^{3+})_{2.0241}O_4$. The Cr_2O_3 and FeO contents of the spinel are 59.95% and 10.7%, respectively. Based on the composition, the spinel is named chromium spinel. The sample was ground under acetone in an agate mortar to an average grain size of 5 μm and dried.

P–V–T experiment

Energy dispersive diffraction experiments on the chromium spinel were carried out in situ at high pressure and temperature in a resistance heated diamond-anvil cell at 4W2 High-Pressure Station of Beijing Synchrotron Radiation Facility (BSRF). The size of the X-ray focal spot is 50 μm × 15 μm and the culet of the DAC is 500 μm. The sample powder was loaded with the inner pressure standard Mo powder into a 200 μm hole in a T301 stainless steel gasket. The pressure medium was a mixture of methanol and ethanol and water with 16:3:1. The pressure in the DAC was determined by using the equation of state of Mo [31]. The samples were heated using a resistance-heating system and temperature was measured by the NiCr–NiSi thermocouple with its precision of ± 2 °C.The diffraction angle(2θ) was set to 12.748°(±0.018°),which was calibrated by the diffractive peaks of Mo at ambient conditions. Details of the experimental technique have been described previously [32].

Typical exposure time for the diffraction patterns was 600 s. Typical spectra at selected pressures and temperatures were shown in Fig. 1. The unit-cell parameters of both spinel and Mo were calculated from peak positions by least squares technique. In the calculation, sample diffraction lines 111,311,400,551, and 440 were used to refine the parameters, and sometimes 220 was also used when available.

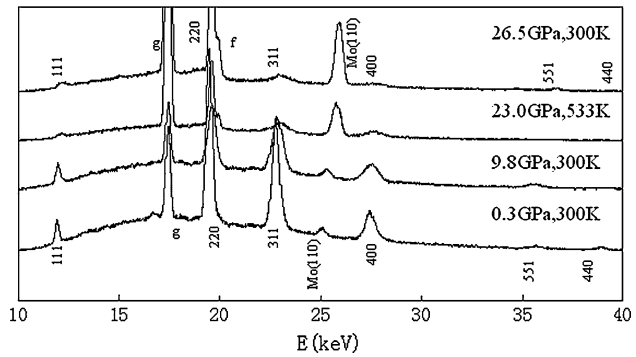

Fig. 1 Representative X-ray diffraction spectra of the chromium spinel under different pressures and temperatures. f—Fluorescence peak of Mo; g—gasket X-ray diffraction peak

Table 1 Cell parameters versus pressure and temperature for the chromium spinel

P (GPa)	T (K)	a (Å)	V (Å^3)	P (GPa)	T (K)	a (Å)	V (Å^3)
0.1	300	8.229(2)	557.32(35)	18.4	353	8.057(1)	523.06(20)
3.1	300	8.194(4)	550.16(43)	7.8	443	8.171(5)	545.45(33)
5.4	300	8.167(3)	544.68(23)	13.0	443	8.117(6)	534.74(23)
9.7	300	8.123(3)	536.03(36)	24.4	443	8.026(2)	517.06(36)
12.2	300	8.095(2)	530.42(28)	7.2	533	8.189(2)	549.16(29)
15.0	300	8.073(4)	526.23(33)	15.4	533	8.103(5)	532.03(36)
16.4	300	8.059(3)	523.36(21)	17.5	533	8.090(3)	529.55(28)
19.8	300	8.028(4)	517.36(33)	22.8	533	8.049(3)	521.53(26)
23.0	300	8.007(3)	513.37(26)	7.8	628	8.195(4)	550.26(34)
26.8	300	7.991(2)	510.29(31)	10.7	628	8.160(2)	543.32(34)
7.3	353	8.163(5)	543.88(21)	18.6	628	8.089(3)	529.35(28)
16.4	353	8.073(4)	526.08(27)	23.4	628	8.055(3)	522.63(23)

Numbers in brackets are 1σ error in last digits

Results and discussion

As pressure increased, all the peaks shifted continuously toward higher energy, but the overall pattern did not change. And all of the diffraction data were obtained inside the stability field of the chromium spinel. Therefore, we suggest that the sample is stable up to 26.8 GPa (Fig. 1). The obtained cell parameters were calculated by using the Unitcell process [33] show a smooth, continuous decrease with increasing pressure (Table 1).

High-temperature Birch-Murnaghan equation of state

The high-temperature Birch-Murnaghan (HTBM) equation of state is often used to fit the P–V–T data. The equation of state is given by the following expression:

$$P = \left(\frac{3}{2}\right) K_0 \left[\left(\frac{V_0}{V}\right)^{\frac{7}{3}} - \left(\frac{V_0}{V}\right)^{\frac{5}{3}}\right] \times \left\{1 + \frac{3}{4}\left(K_0' - 4\right)\left[\left(\frac{V_0}{V}\right)^{\frac{2}{3}} - 1\right]\right\}, \quad (1)$$

where V_0, K_0, K_0' are the zero-pressure volume, isothermal bulk modulus, and its pressure derivative, respectively.

In the first approach, Eq. 1 is modified to take into account the effects of temperature dependence of the bulk modulus:

$$K_T = K_0 + \left(\frac{\partial K}{\partial T}\right)_P (T - 300), \quad (2)$$

and the cell volume

$$V_T = V_0 \exp \int_{300}^{T} \alpha_T \mathrm{d}T, \quad (3)$$

where $\left(\frac{\partial K}{\partial T}\right)_P$ is the temperature derivative of the bulk modulus, which is assumed to be constant over the whole temperature range, and α_T is the thermal expansivity at ambient pressure.

We assume that K_T' does not change with temperature, i.e. $\left(\frac{\partial K_T'}{\partial T}\right)_P = 0$. The experimental P–V–T data were fitted to high-temperature Birch-Murnaghan (HTBM) EOS (Fig. 2). Using our measured $V_0 = 557.86$ Å^3, we obtained that

$$K_0 = 209 \pm 9\,\mathrm{GPa}, \quad K_0' = 7 \pm 1,$$
$$K_0'' = -0.0933\,\mathrm{GPa}^{-1},$$
$$\left(\frac{\partial K}{\partial T}\right)_P = -0.056 \pm 0.035\,\mathrm{GPa\,K}^{-1},$$
$$\alpha_0 = 7 \pm 1 \times 10^{-5}\mathrm{K}^{-1}$$

Discussion

So far, many experimental studies of the elastic properties of spinel have been conducted [14–30]. Their bulk moduli (K_0) and pressure derivatives (K_0') are listed in Table 2.

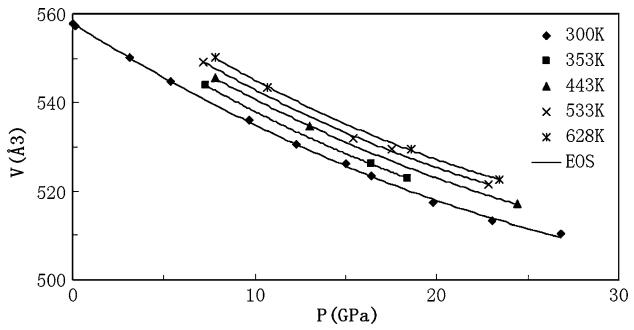

Fig. 2 P–V–T data of the chromium spinel. The solid lines are isothermal Birch-Murnaghan fits at temperatures 300, 373, 473, and 573 K, respectively

Among spinels, $MgAl_2O_4$ is one of the most common spinels, and both its high-temperature and high-pressure behavior has been studied intensively [14–18]. Various reports on the K_0 of $MgAl_2O_4$ converge to $K_0 = 190$–198 GPa (Table 2). Catti et al. [19] had studied the high-pressure equation of state of chromium spinel ($MgCr_2O_4$, $MnCr_2O_4$, and $ZnCr_2O_4$) by theoretical calculations, and the bulk modulus of $MgCr_2O_4$, $MnCr_2O_4$, and $ZnCr_2O_4$ are 197.3, 205.8, and 215.0 GPa, respectively. The studies of $MgFe_2O_4$ give K_0 value in the range from 181.5 to 190 GPa [20]. Levy et al. [21] have investigated the structural behavior of synthetic gahnite ($ZnAl_2O_4$) by X-ray powder diffraction, and they obtained the bulk modulus of $ZnAl_2O_4$ as 201.7 GPa. Levy et al. [22] also measured the elastic properties of synthetic zincochromite ($ZnCr_2O_4$), and the bulk modulus of $ZnCr_2O_4$ is 183.1 GPa. The bulk modulus of the same end-member compositions of spinel ($ZnCr_2O_4$) determined by X-ray diffraction at high pressure is about 15% lower than that of Catti et al., which was determined by theoretical calculations. The investigation of $ZnFe_2O_4$ indicated that K_0 value is 166 GPa [23]. Recently, several authors also have studied the compressibility of $FeAl_2O_4$, $FeCr_2O_4$, and $FeFe_2O_4$ (Table 2) [16, 24–29].

The compressibility of the $MgCr_2O_4$ and $MgFe_2O_4$ is very similar to that of $MgAl_2O_4$, while the $ZnAl_2O_4$ is less compressible than $ZnFe_2O_4$. But, according to the electronic configurations involved, the $ZnFe_2O_4$ is always softer than $ZnAl_2O_4$. The bulk modulus values obtained from FeAl- and ZnAl-spinels are in general higher than the MgAl compositions. So, Levy et al. [15] claimed that the main reason of the relatively large bulk modulus of $ZnAl_2O_4$ was the Zn^{2+} cation replacing Mg^{2+} cation in the tetrahedral site, supported by Levy et al. [23] who considered that the replacement of Fe^{2+} with Zn^{2+} brought the elastic properties of franklinite significantly different from those of magnetite.

From Table 2, the bulk modulus of the chromium spinel in this study is slightly larger than those in previous studies, whereas in good agreement with Reichmann et al. [34]. There are two possible sources for the high bulk modulus.

First, we used a methanol–ethanol–water mixture with 16:3:1 for the pressure medium, which freezes above 10 GPa, and the hydrostatic circumstance of sample chamber will be influenced [35]. In this study, the bulk modulus obtained from the hydrostatic conditions (up to 9.7 GPa), $K_0 = 207(6)$ GPa, is smaller than the experimental measurements of elastic modulus that lead to $K_0 = 209(9)$ GPa. This difference is very likely related to the different experimental conditions (hydrostaticity and non-hydrostaticity condition). Fei et al [36] considered that the bulk modulus derived from compression data under nearly hydrostatic conditions was smaller than from non-hydrostatic compression data. So, we infer that the non-hydrostatic condition may be a reason, but not a primary reason, for the relatively large bulk modulus.

Table 2 Parameters comparison of the equation of state of spinel

Reference	Sample	K_0 (GPa)	K'_0	$(\partial K/\partial T)_P$ ($GPaK^{-1}$)
BM[a]	$Mg_{0.95(4)}Al_{2.03(3)}O_4$	190.8(1.2)	6.77(15)	–
BM[b]	$Mg_{0.94}Al_{2.04}O_4$	190(2)	4.0(fixed)	–
	$Mg_{0.94}Al_{2.04}O_4$	195(7)	2.2(2)	–
BM[c]	$MgAl_2O_4$	196(1)	4.7(3)	–
BM[d]	$MgAl_2O_4$	194(6)	4.0(fixed)	–
UM[e]	$MgAl_2O_4$	197.9		–
BM[f]	$MgFe_2O_4$	181.5(1.3)	6.32(14)	–
HF[g]	$MgCr_2O_4$	197.3	3.94	–
	$MnCr_2O_4$	205.8	3.67	–
	$ZnCr_2O_4$	215.0	3.96	–
BM[h]	$ZnAl_2O_4$	201.7(9)	7.62(9)	–
BM[i]	$ZnFe_2O_4$	166.4(3.0)	9.3(6)	–
BM[j]	$ZnCr_2O_4$	183.1(3.5)	7.9(6)	–
UM[k]	$FeAl_2O_4$	210.3		–
[l]	$FeCr_2O_4$	203.3		–
BM[m]	$FeFe_2O_4$	183(10)	4.0(fixed)	–
BM[n]	$FeFe_2O_4$	215(25)	7.5(4)	–
BM[o]	$FeFe_2O_4$	217(2)	4.0(fixed)	–
UM[p]	$FeFe_2O_4$	185.7(3.0)	5.1(1)	–
UM[q]	$(Zn^{2+}Fe^{2+}Mg^{2+})_{0.9672}(Al^{3+})_{1.99}O_4$	209(5)	4.8(3)	–
BM[r]	$(Na^{+}Mg^{2+}Fe^{2+}Ti^{4+})_{0.9672}(Cr^{3+}Al^{3+})_{2.0234}O_4$	369	4.0(fixed)	–
BM[s]	$(Na^{+}Mg^{2+}Fe^{2+}Ti^{4+})_{0.9661}(Cr^{3+}Al^{3+})_{2.0241}O_4$	209(9)	7(1)	−0.056(35)

Notes: BM = Bird-Murnaghan EOS; M = Murnaghan EOS; HF = Hartree-Fock; UM = Ultrasonics methods; [a] Levy et al. [15]; [b] Pavese et al. [17a]; [c] Kruger et al. [14]; [d] Finger et al. [16]; [e] Yoneda [18]; [f] Levy et al. [20]; [g] Catti et al. [19]; [h] Levy et al. [21]; [i] Levy et al. [23]; [j] Levy et al. [22]; [k] Wang and Simmons [24]; [l] Hearmon [25]; [m] Mao et al. [26]; [n] Gerward and Staun Olsen [27]; [o] Haavik et al. [28]; [p] Reichmann and Jacobsen [29]; [q] Reichmann and Jacobsen [34]; [r] Ma et al. [30]; [s] This work. Numbers in brackets are 1σ error in last digits

Second, the sample of this experiment has high content of the FeO. The Fe^{2+} cation is believed to replace to the Mg^{2+} cation in the tetrahedral site in the natural chromium spinel. According to discussed by Vermaas and Schmidt [37], in the spinels the degree of covalence in bonds increases with increasing Fe^{2+} content. Moreover, the pressure derivative of Fe^{2+}–O bonds (49×10^4 Å/GPa) is much greater than Mg^{2+}–O bonds (46×10^4 Å/GPa) [38]. A comparison between the elastic parameters in this work and in previous results of $MgAl_2O_4$, $MgCr_2O_4$, $FeAl_2O_4$, and $FeCr_2O_4$ reveals that the responsibility for bulk modulus of Fe^{2+}–Mg^{2+} substitution in tetrahedral site is more than Cr^{3+}–Al^{3+} substitution in octahedral site. Therefore, we suggest that although the effect of non-hydrostaticity exists and the Fe^{2+} cation replacing the Mg^{2+} cation in the tetrahedral site are the main reason for the relatively large bulk modulus in our experiment. Our conclusions approve the above views about the effect of chemical substitution to bulk modulus in end-member spinels.

Conclusion

The P–V–T measurements on chromium spinel at pressures up to 26.8 GPa in the temperature range of 300–628 K were carried out using RHDAC technique. The isothermal bulk modulus, and its pressure derivative, the temperature derivative of the bulk modulus and the thermal expansivity coefficient of the natural chromium spinel are 209 ± 9 GPa, 7 ± 1, -0.056 ± 0.035 GPa K^{-1}, $7 \pm 1 \times 10^{-5}$ K^{-1}, respectively. The temperature derivative of the bulk modulus $(\partial K/\partial T)_P$ is obtained for the first time. The main reason of the relatively large bulk modulus of the natural chromium spinel is the Fe^{2+} cation replacing Mg^{2+} cation in the tetrahedral site.

Acknowledgements We thank two anonymous referees for their helpful comments and suggestions. This work was performed at 4W2 High-Pressure Station, Beijing Synchrotron Radiation Facility (BSRF). High-Pressure Station is supported by Chinese Academy of Sciences (Grant No. KJCX2-SW-N20,KJCX2-SW-N03). This work is supported by National Basic Research Program of China (Grant No 2005CB724400), the Knowledge Innovation Project of Chinese Academy of Science (Grant No KJCX2-SW-N20), and the National Natural Science Foundation of China (Grant No 40574036).

References

1. Ueda N, Omata T, Hikuma N, Ueda K, Mizoquchi H, Hashimoto T et al (1992) Appl Phys Lett 61:1954. doi:10.1063/1.108374
2. McCallum RW, Johnston DC, Luengo CA, Maples MB (1976) J Low Temp Phys 25:177. doi:10.1007/BF00654828

3. Gusmano G, Montesperelli G, Nunziante P, Traversa E (1993) Br Ceram Trans 92:104
4. Wakamura K (1989) J Solid State Chem 78:197. doi:10.1016/0022-4596(89)90096-0
5. Green HWII (1984) Geophys Res Lett 11:817. doi:10.1029/GL011i009p00817
6. Arai S (1992) Mineral Mag 56:173. doi:10.1180/minmag.1992.056.383.04
7. Irifune T, Fujino K, Ohtani E (1991) Nature 349:409. doi:10.1038/349409a0
8. Funamori N, Jeanloz R, Nguyen JH, Kavner A, Caldwell WA (1998) J Geophys Res 103:20813. doi:10.1029/98JB01575
9. Liu LG (1978) Earth Planet Sci Lett 41:398. doi:10.1016/0012-821X(78)90171-1
10. Irifune T, Naka H, Sanchira T, Inoue T, Funakoshi K (2002) Phys Chem Miner 29:645. doi:10.1007/s00269-002-0275-1
11. Akaogi M, Hamada Y, Suzuki T, Kobayashi M, Okada M (1999) Phys Earth Planet Inter 115:67. doi:10.1016/S0031-9201(99)00076-X
12. Wang ZW, Lazor P, Saxena SK, O'Neill Hugh St C (2002) Mater Res Bull 37:1589
13. Andrault D, Bolfan-Casanova N (2001) Phys Chem Miner 28:211. doi:10.1007/s002690000149
14. Kruger MB, Nguyen JH, Caldwell W, Jeanloz R (1997) Phys Rev B 56:1. doi:10.1103/PhysRevB.56.1
15. Levy D, Pavese A, Hanfland M (2003) Am Mineral 88:93
16. Finger LW, Hazen RM, Hofmeister AM (1986) Phys Chem Miner 13:215. doi:10.1007/BF00308271
17. (a) Pavese A, Artioli G, Hull S (1999) Am Mineral 84:905; (b) Nestola F, Ballaran B, Balic-Zunic T, Princivalle F, Secco L, Negro AD (2007) Am Mineral 92:1838
18. Yoneda A (1990) J Phys Earth 38:19
19. Catti M, Fava FF, Zicovich C, Dovesi R (1999) Phys Chem Miner 26:389
20. Levy D, Diella V, Dapiaggi M, Sani A, Gemmi M, Pavese A (2004) Phys Chem Miner 31:122
21. Levy D, Pavese A, Sani A, Pischedda V (2001) Phys Chem Miner 28:612
22. Levy D, Diella V, Pavese A, Dapiaggi M, Sani A (2005) Am Mineral 90:1157
23. Levy D, Pavese A, Hanfland M (2000) Phys Chem Miner 27:638
24. Wang D, Simmons G (1972) J Geophys Res 77:4379
25. Hearmon RFS (1984) In: Hellwege KH, Hellwege AM (eds) Landolt-Börnstein Tables, III/18. Springer Verlag, Berlin, p 559
26. Mao HK, Takahashi T, Bassett WA, Kinsland GL, Merrill L (1974) J Geophys Res 79:1165
27. Gerward L, Staun Olsen J (1995) Appl Radiat Isot 46:553
28. Haavik C, Stolen S, Fjellvag H, Hanfland M, Häusermann D (2000) Am Mineral 85:514
29. Reichmann HJ, Jacobsen SD (2004) Am Mineral 89:1061
30. Ma MN, Liu J, Zhou WG, Li YC, Li XD (2004) Nucl Technol 27:931 in Chinese
31. Zhao YS, Lawson AC, Zhang JZ, Bennett BI (2000) Phys Rev B 62:8766
32. Liu J, Zhao J, Che RZ, Yang Y (2000) Chin J High Press Phys 14:247 in Chinese
33. Holland TJ, Tedfern SA (1997) Mineral Mag 61:65
34. Reichmann HJ, Jacobsen SD (2006) Am Mineral 91:1049
35. Piermarini GJ, Block S, Barnett JD (1973) J Appl Phys 44:5377
36. Fei YW (1999) Am Mineral 84:272
37. Vermaas FHS, Schmidt ER (1959) B Miner Petrol 6:219
38. Hazen RM, Yang HX (1999) Am Mineral 84:1956